ESC HEART FAILURE
ESC Heart Failure 2024; **11**: 1205–1217
Published online 30 January 2024 in Wiley Online Library (wileyonlinelibrary.com) **DOI:** 10.1002/ehf2.14673

ORIGINAL ARTICLE

CircRbms1 fosters MST1 mRNA and protein levels to motivate myocardial ischaemia–reperfusion injury via autophagic status

Qin Liu[1], Guorong Lai[2], Yanhui Hu[1], Fan Yang[2], Chao Zhang[2], Dongsheng Le[2], Fumou Deng[1], Xianliang Xing[1], Binquan Tang[1], Huanhuan Jie[3], Yingping Liang[2]* and Enjun Lei[4]*

[1]*Department of Anesthesiology, the 2nd affiliated hospital, Jiangxi Medical College, Nanchang University, Nanchang, China;* [2]*Department of Pain Management, the 2nd affiliated hospital, Jiangxi Medical College, Nanchang University, Nanchang, China;* [3]*Department of Anesthesiology, Ganzhou People's Hospital, Ganzhou, China; and* [4]*Department of Anesthesiology, First Affiliated Hospital of Nanchang University, Nanchang, China*

Abstract

Aims Acute myocardial infarction (MI) is a significant contributor to death in individuals diagnosed with coronary heart disease on a worldwide level. The specific mechanism by which circRbms1 contributes to the damage caused by myocardial ischaemia–reperfusion (I/R) is not well understood. The primary aim of this study was to examine the role of circRbms1 and its associated mechanisms in the setting of I/R injury.

Methods and results An in vivo MI mice model and an in vitro MI cell model was established. The expression levels were detected using quantitative real-time PCR (qRT-PCR) and western blot. Cellular proliferation, apoptosis, pyroptosis, and autophagy were detected by immunostaining, immunohistochemistry, western blot, and transmission electron microscopy (TEM). Dual-luciferase reporter assay, RNA pull-down assay, and RIP assay were performed to validate the molecular interactions. CircRbms1 was up-regulated in A/R-induced HCMs and acted as a sponge for miR-142-3p, thereby targeting MST1. CircRbms1 could improve stability of MST1 by recruiting IGF2BP2 (all $P < 0.05$). CircRbms1 knockout reduced cell pyroptosis, improved autophagy and proliferation level in A/R-induced HCMs (all $P < 0.05$). CircRbms1 knockout alleviated cardiac dysfunction and cell pyroptosis and enhanced autophagy and proliferation in mice through the miR-142-3p/MST1 axis.

Conclusions CircRbms1 inhibited the miR-142-3p/MST1 axis and played a protective role in myocardial I/R injury. It may provide a new therapeutic target for I/R heart injury.

Keywords Autophagy; circRbms1; miR-142-3p; MST1; Myocardial injury; Pyroptosis

Received: 22 August 2023; Revised: 29 November 2023; Accepted: 18 December 2023
**Correspondence to: Enjun Lei, Department of Anesthesiology, First Affiliated Hospital of Nanchang University, No. 17, Yongwai Street, Donghu District, Nanchang 330006, Jiangxi Province, China. Email: enjunlei26@163.com;*
Yingping Liang, Department of Pain Management, the 2nd affiliated hospital, Jiangxi Medical College, Nanchang University, No. 1, Minde Road, Donghu District, Nanchang 330006, Jiangxi Province, China. Email: liangyingping413@163.com
Qin Liu and Guorong Lai are co-first authors.

Introduction

Acute myocardial infarction (MI) is one of the most common and critical conditions in hospital and also one of the main causes of death in patients with coronary heart disease worldwide. Timely reperfusion therapy is an effective way to relieve myocardial ischaemia and reduce infarct size, but it also causes irreversible damage to the myocardium and coronary circulation, namely, myocardial ischaemia–reperfusion (I/R) injury, which is a key factor affecting the prognosis of MI patients.[1] I/R injury involves multiple cellular and molecular mechanisms, including autophagy, apoptosis, necrosis, necroptosis, inflammation, oxidative stress, and calcium overload.[2] I/R injury not only affects cardiomyocytes but also affects the coronary microcirculation, leading to microvascular obstruction (MVO), which further aggravates myocardial ischaemia and cardiac dysfunction.[3] Therefore, it is of great significance to understand the pathogenesis of I/R injury and find effective cardioprotective strategies for improving the clinical outcomes of MI patients. Currently, various

© 2024 The Authors. ESC Heart Failure published by John Wiley & Sons Ltd on behalf of European Society of Cardiology.
This is an open access article under the terms of the Creative Commons Attribution-NonCommercial License, which permits use, distribution and reproduction in any medium, provided the original work is properly cited and is not used for commercial purposes.

mechanical and pharmacological interventions have been proven to reduce I/R injury in animal models, such as ischaemic preconditioning, ischaemic postconditioning, remote ischaemic conditioning, and targeted drugs.[4] However, these methods are not satisfactory in clinical trials, which may be related to the patient's age, co-morbidities, medication treatment, and so on. Therefore, there is an urgent need to explore more effective and safe cardioprotective methods and consider their impact on long-term targets such as MVO, myocardial repair, and reverse remodelling.

Circular RNAs (circRNAs) are a class of non-coding RNAs that are formed by back-splicing of exons or introns. CircRNAs are widely expressed in various tissues and cell types and have diverse functions in regulating gene expression, protein translation, RNA splicing, and interacting with RNA-binding proteins.[5] CircRNAs have been implicated in various pathological processes, including I/R injury.[6] Among them, myocardial I/R injury is a major contributor to morbidity and mortality in patients with acute myocardial infarction (AMI), which is characterized by irreversible loss of cardiomyocytes and impaired cardiac function.[2] CircRNA single stranded interacting protein 1 (circRbms1) was found to be up-regulated in myocardial I/R injury and to promote cardiomyocyte apoptosis by sponging miR-2355-3p and up-regulating its target gene mammalian sterile20-like kinase 1 (MST1), which is a pro-apoptotic kinase that mediates mitochondrial dysfunction and oxidative stress. Knockout of circRbms1 played a protective role in myocardial I/R injury though inhibition of miR-2355-3p/MST1 axis.[7] This finding suggests that circRbms1 may be a potential therapeutic target for myocardial I/R injury. However, the role of circRbms1 in myocardial I/R injury is not fully understood. Therefore, further studies are needed to elucidate the comprehensive functions and mechanisms of circRbms1 in myocardial I/R injury.

Pyroptosis is a novel form of programmed cell death that is characterized by gasdermin D-mediated plasma membrane rupture and inflammatory cytokine release. Pyroptosis has been implicated in various cardiovascular diseases, including myocardial I/R injury.[8] However, the molecular mechanisms and therapeutic targets of cardiomyocyte pyroptosis in myocardial I/R injury remain elusive. Autophagy is a lysosomal degradation pathway that maintains cellular homeostasis and survival under stress conditions. Autophagy can also modulate cell death pathways, such as apoptosis and necroptosis, by regulating the turnover of key proteins and organelles.[9] However, the role of autophagy in cardiomyocyte pyroptosis and its interaction with other cell death pathways in myocardial I/R injury is poorly understood.

In this study, we aimed to investigate the potential regulation and function of circRbms1 on the link between autophagy and pyroptosis of cardiomyocytes, either with its other possible downstream machinery to be involved in the pathogenesis of myocardial I/R injury, thereby providing novel intervention and therapeutic targets.

Materials and methods

Animal experiment

The following four groups were randomly divided into by 8-week male C57BL/6 mice (20–26 g): (1) I/R + sh-NC group; (2) I/R + shcircRbms1 group; (3) I/R + shcircRbms1 + anti-miR-142-3p group; (4) I/R + shcircRbms1 + MST1 group (five mice for each group). The surgical procedure reported in Zhang et al.[10] was followed. The mice were anaesthetized with 2% isoflurane inhalation and artificially ventilated (80 strokes/min). The chest was opened at the fourth intercostal space, and the heart and the left anterior descending artery (LAD) were exposed. The LAD was ligated with a 7–0 silk suture and reperfused 45 min later and lasted for 3 h. Adenoviruses vectors to inhibit circRbms1 were injected through tail vein. Five days after adenovirus administration, the following experiments were performed. International guidelines for animal research projects were obeyed, and the approval from the Animal Ethics Committee of First Affiliated Hospital of Nanchang University was obtained.

Cell culture and a/R-induced cell injury

RPMI-1640 containing 10% FBS, 100 μg/mL streptomycin, and 100 U/mL penicillin was used to culture primary human cardiac myocytes (HCMs, American Type Culture Collection, ATCC; Manassas, VA, USA) at 37°C with 95% air and 5% CO_2. A hypoxia chamber with an anerobic pouch under 5% CO_2/95% N_2 was used to culture HCMs for 24 h followed with reoxygenation at 37°C with 5% CO_2 for 3 h to establish the model of A/R-induced cell injury.

Cell transfection

miR-142-3p mimic, miR-142-3p inhibitor (termed anti-miR-142-3p), and its negative controls were designed and synthesized by RiboBio (Guangzhou, China). Adenoviruses vectors to inhibit circRbms1 were constructed (lenti-sh-circRbms1) and lenti-sh-circRbms1 or lenti-sh-NC (100 μL), synthesized by HanBio Biotechnology Co., Ltd (Shanghai, China). Additionally, the full-length sequences of MST1 were cloned into the pcDNA3.1 vector to obtain the corresponding pcDNA3.1-MST1 overexpression plasmids. Transfection of above-mentioned plasmids was conducted with Lipofectamine 3000 (Invitrogen, CarIsbad, CA), and these cells were used for subsequent experiments.

Ki67 detection

HCMs were fixed, permeabilized, blocked, and incubated with primary antibody against Ki67 (clone SP6, Thermo Fisher

Scientific). After washing, secondary antibody conjugated to Alexa Fluor 488 (Thermo Fisher Scientific) was added. Cells were mounted with DAPI (Thermo Fisher Scientific) and imaged. Ki67-positive cells percentage was calculated by dividing Ki67-positive nuclei by DAPI-stained nuclei.

Transmission electron microscope

Fixation of cells with 2.5% glutaraldehyde in 0.1 M cacodylate buffer (pH 7.4) was performed for 2 h at room temperature. Cacodylate buffer was used to wash the cells, which were then postfixed with 1% osmium tetroxide for 1 h and dehydrated in ethanol. Epoxy resin was used to embed and polymerize the cells at 60°C for 48 h. A diamond knife was used to cut ultrathin sections (70 nm), which were stained with uranyl acetate and lead citrate. A transmission electron microscope was used to examine the sections, and a digital camera was used to capture the images. Double-membrane vesicles with cytoplasmic material were identified as autophagosomes.

RIP assay

Lysis of cells in RIP buffer with protease and RNase inhibitors was performed. Protein A/G beads were used to preclear the cell lysates and then incubate with an antibody against IGF2BP2 (Cell Signaling Technology, 64143) or IgG (Abcam, ab96899) overnight at 4°C. The antibody-RBP complexes were captured by protein A/G beads and washed with RIP buffer. TRIzol reagent was used to extract RNA from the beads and reverse transcribe it into cDNA. The enrichment of indicated gene was measured by qRT-PCR analysis.

Subcellular fractionation

Fractionation buffer (20 mmol HEPES (pH 7.5), 10 mmol KCl, 1.5 mmol MgCl2, 1 mmol EGTA, 1 mmol EDTA, 1 mmol DTT, and 0.1 mmol phenylmethanesulfonyl fluoride), 250 mmol sucrose, and 20 mmol protease inhibitor cocktail (Sigma-Aldrich, St. Louis, MO, USA) were used to wash and resuspend the cells. A Dounce homogenizer was used to homogenize the cell suspension, and the nuclei were pelleted by centrifuging at 750× *g* for 5 min. The supernatant containing the cytosolic and ER fraction was centrifuged at 10 000× *g* for 15 min to pellet the mitochondrial fraction. The cytosolic fraction was obtained by centrifuging the supernatant again. qRT-PCR was used to analyse the expression in the fractions.

Fluorescent in situ hybridization (FISH)

FITC-labelled circRbms1 and Cy3-labelled IGF2BP2 probes were utilized for assessing the colocalization of circRbms1 and IGF2BP2 in cells. Briefly, cells were fixed and mounted on glass slides. The FISH assay was subsequently conducted using the Fluorescent In Situ Hybridization Kit (Geneseed, Guangzhou, China) following the manufacturer's protocol. Fluorescent probes against circRbms1 and IGF2BP2 were added to the slides and allowed to hybridize with the complementary DNA sequence on the chromosomes. The excess probe was washed away, and the slides were examined under a fluorescence microscope.

Actinomycin D treatment

Cells were treated with Actinomycin D (5 μg/mL, R&D, Minneapolis, MN, USA) for 60 min to several hours, and RNA was extracted using TRIzol reagent. mRNA levels of MST1 were measured by qRT-PCR.

RNA pull-down assay

The streptavidin magnetic beads (Cat. No. HYK0208, MedChemExpress) were incubated with the biotinylated circRbms1 probe or the oligo probe (RiboBio) as the control at room temperature for 2 h. The circRbms1 probe or the oligo probe was mixed with lysed HCMs (1×10^7) at 4°C overnight. Trizol was used to conduct the extraction of bound RNA and qRT-PCR was performed to detect RNA.

Echocardiographic assessment

Evans blue dye (1 mL of a 2% solution; Sigma-Aldrich) was injected through jugular vein to delineate the ischaemic area at risk after reperfusion. The mice were euthanized by cervical dislocation, and the heart was excised and sectioned. The heart slices were incubated with 1.0% 2,3,5-triphenyltetrazolium chloride (TTC; Sigma-Aldrich) for 15 min at 37°C to differentiate live (red) and dead or infarcted myocardium (white). Ice-cold sterile saline was used to wash the slices, which were fixed in 10% formaldehyde, weighed, and photographed from both sides. Computer-assisted planimetry was used by a blinded histologist to assess the infarct area (INF) and the risk zone. The INF/LV ratio (%) was calculated.

Luciferase reporter assay

The pGL3 vector (Hunan Fenghui Biotechnology Co., Ltd) was inserted with circRbms1 3′-UTR or MST1 3′-UTR with/without

the predicted responsive element of miR-142-3p (circRbms1-WT, circRbms1-MUT, MST1-WT, and MST1-MUT) that were amplified. The luciferase reporter vectors and miR-142-3p mimics or NC control (Biomics Biotech) were transfected into samples using Lipofectamine 3000 (Invitrogen). A TransDetect® Double-Luciferase Reporter Assay Kit (FR201-01, TransGen Biotech Co., Ltd.) was used to analyse the luciferase activity at 48 h after the transfection and the value of Renilla luciferase activity was used to normalize it.

Quantitative real-time PCR (qRT-PCR)

TRIzol reagent (Invitrogen) was used to conduct extraction of total RNA from HCMs and tissues. TransScript First-Strand cDNA Sythesis SuperMix was used to reversely transcribe 2 μg of template RNA into cDNA for miRNA quantification. The Thermal Cycler Dice Real-Time System II (Takara) was used to perform the fluorescence quantitative PCR reaction. PrimeScript™ One Step qRT-PCR kit (Takara) was applied for reverse transcription from RNA into cDNA for quantification of circRbms1 or MST1. An ROX Reference Dye II (GenStar) on StepOnePlusTM Real-Time PCR System (Applied Biosystems) was used to perform the PCR reactions. The following primer sequences were used in qPCR: U6 forward 5′-CTCGCTTCGGCAGCACA-3′ and reverse 5′-AACGCTTCACGAATTTGCGT-3′; GAPDH forward 5′-CACCAGGGCTGCTTTTAACTC-3′ and reverse 5′-TGGAAGATGGTGATGGGATTT-3′; circRbms1: forward 5′-CCCTGATCTCCATACCCAGA-3′ and reverse 5′-TGGAGTCGAGTGTTTGCAGT-3′; MST1 forward 5′-AGACCTCCAGGAGATAATCAAAGA-3′ and reverse 5′-AGATACAGAACCAGCCCCACA-3′. GAPDH and U6 were used to normalize the expression of mRNA and miRNA, respectively. Data were analysed by using the $2^{-\Delta\Delta Ct}$ method.

Western blot

PVDF membranes were transferred with 12% SDS-PAGE and blocked with 5% defatted milk. Primary antibodies were incubated with the protein samples at 4°C overnight followed by incubation of secondary antibody goat anti-rabbit IgG H&L preadsorbed (Abcam, ab96899, 1/1000) at 37°C for 45 min. MST1 antibody (Abcam, ab245190, 1/1000), cleaved caspase-1 antibody (Cell Signaling Technology, 89332, 1/1000), NLRP3 antibody (Cell Signaling Technology, 15101, 1/1000), beclin1 (Abclonal, A7353, 1:2000), LC3 (Cell Signaling Technology, 4108, 1:2000), p62 (Abcam, ab91526, 1:1000), and MST1 antibody (Abcam, ab245190, 1/1000) were the primary antibodies used. β-Actin was used as the control. Chemiluminescence reagents were used to visualize protein bands and ImagePro plus software 6.0 was used to quantify them.

Immunofluorescence

Fixation of cells with 4% formaldehyde was performed, and then they were washed three times using iced PBS. Next, cell permeabilization was achieved by using PBS with 0.25% Triton X-100 and another three washes with iced PBS followed. Primary anti-caspase-1 antibody (Abcam, ab138483, 1:200), anti-LC3II antibody (Abcam, ab192890, 1:200), and anti-Ki67 antibody (Abcam, ab15580, 1:200) were added to the cells, and they were incubated overnight at 4°C. Then, secondary antibody (LS-C60498, 1/1000, LSBio) was supplemented to the samples, and a 2-h incubation at room temperature was done. Finally, the samples were mounted and imaged by a confocal microscope.

Data analysis

Mean ± standard deviation (SD) was used to display all data. Student's *t*-test was applied for comparison of two groups. Graphpad Prism 6.0 software was used for the analysis and graphing of all data. Significance was considered when $P < 0.05$. All experiments were repeated at least three times.

Results

Scheme illustrating the production of circRbms1

Our analysis of circRbms1 across different species using the BLAST website (https://blast.ncbi.nlm.nih.gov/) revealed good conservation between human and mouse sources (*Figure 1A*). Genomic information showed that circRbms1 is derived from exons 10, 11, 12, 13, and 14 of the parental Rbms1 gene (*Figure 1B*). qRT-PCR analysis of the abundance of circRbms1 and Rbms1 in cardiomyocytes treated with RNase R indicated that circRbms1 was more tolerant to RNase R digestion than its linear counterpart Rbms1 (*Figure 1C*). Furthermore, qRT-PCR analysis revealed that circRbms1 was significantly up-regulated in a mouse model of I/R (*Figure 1D*). These results suggested a potential role for circRbms1 in the response to I/R injury.

CircRbms1 serves as a miRNA sponge for miR-142-3p to enhance MST1 expression

To determine the subcellular localization of circRbms1, we performed qRT-PCR analysis on the nuclear and cytoplasmic fractions of cardiomyocytes. Our results showed that circRbms1 was presented in both compartments, with a higher abundance in the cytoplasm (*Figure 2A*). Further investigation into the function of circRbms1 revealed its binding to miR-142-3p through a RNA pull-down assay (*Figure*

Figure 1 Scheme illustrating the production of circRbms1. (A) The conservation of circRbms1 between human and murine was compared in NCBI. (B) Genomic information of circRbms1. (C) The abundance of circRbms1 and Rbms1 in cardiomyocytes treated with or without RNase R was detected by qRT-PCR. (D) CircRbms1 was detected in sham or I/R mouse models (N = 5 per group). Data are presented as mean ± SD from three independent experiments. ***$P < 0.001$.

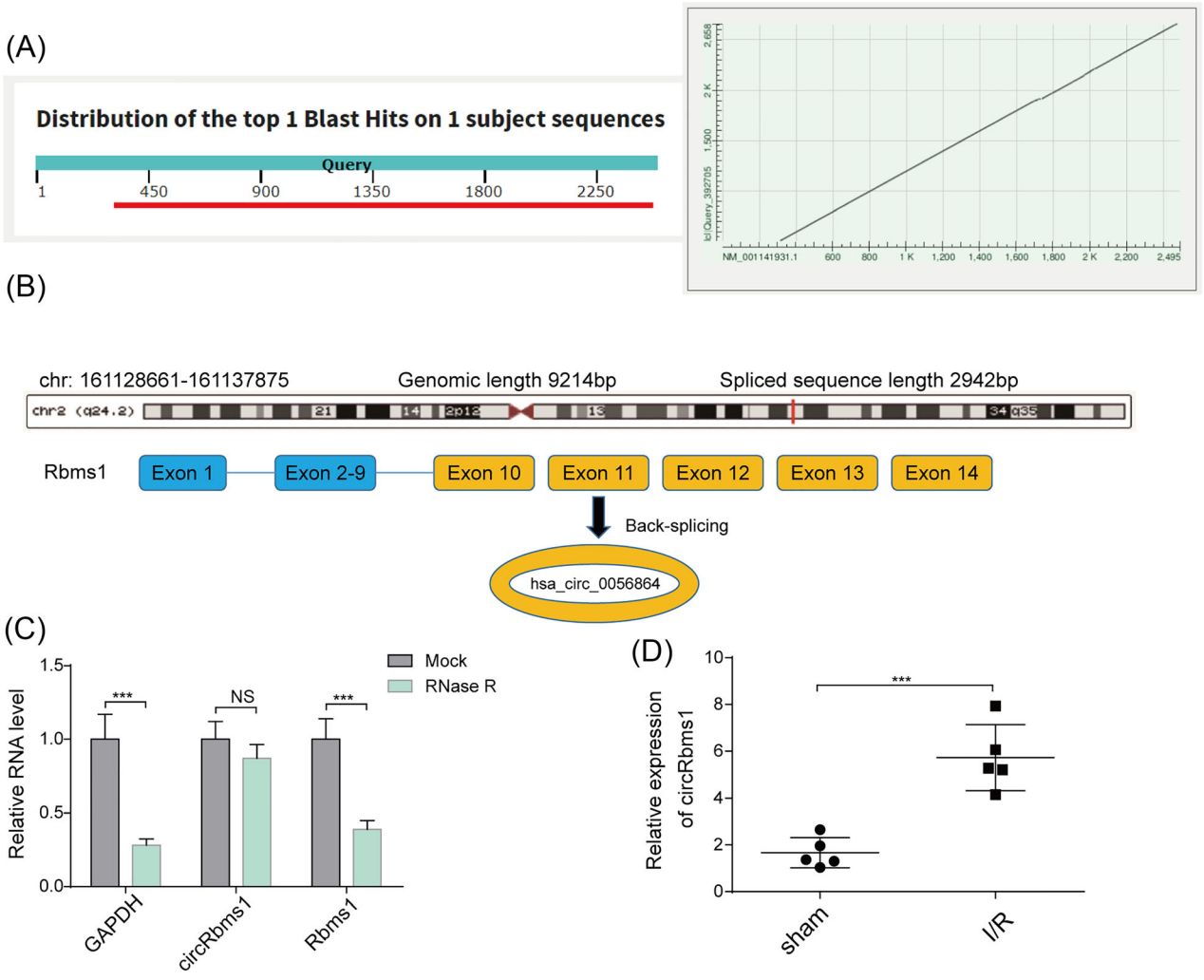

2B). Analysis using CircInteractome identified complementary binding sites between circRbms1 and miR-142-3p. The targeting relationship between the two was validated using a luciferase reporter assay (*Figure 2C*). We also found that circRbms1 negatively regulated the expression level of miR-142-3p through qRT-PCR analysis (*Figure 2D*). Complementary binding sites between miR-142-3p and MST1 were identified using miRDB. A luciferase reporter gene assay confirmed the targeting relationship between the two (*Figure 2E*). qRT-PCR analysis further revealed that miR-142-3p negatively regulated the expression level of MST1 (*Figure 2F*). The binding of miR-142-3p with circRbms1 and MST1 was demonstrated through a RNA pull-down assay (*Figure 2G*). To investigate the effect of circRbms1 on MST1 expression, we performed qRT-PCR and western blot analysis. Our results showed that silencing of circRbms1 inhibited MST1 expression. However, this effect was reversed when miR-142-3p expression was inhibited (*Figure 2H,I*). These findings suggested a potential regulatory role for circRbms1 in MST1 expression via its interaction with miR-142-3p.

Loss of CircRbms1 protects cardiomyocytes against A/R-induced pyroptosis via targeting miR-142-3p/MST1 axis

We performed qRT-PCR analysis to determine the expression levels of circRbms1, miR-142-3p, and MST1 over time. Our results showed that circRbms1 expression increased over time (*Figure 3A*), while miR-142-3p expression decreased over time (*Figure 3B*). MST1 expression increased over time (*Figure 3C*). Immunofluorescence (IF) detection of caspase-1

Figure 2 CircRbms1 serves as a miRNA sponge for miR-142-3p to enhance MST1 expression. (A) The abundance of circRbms1 in the nuclear and cytoplasmic fractions of cardiomyocytes was detected by qRT-PCR analysis. (B) The interaction between circRbms1 and miRNAs was screened by pull down assay. (C) CircInteractome predicted the complementary binding sites of circRbms1 and miR-142-3p, and the targeting relationship was validated by luciferase reporter assay. (D) The abundance of circRbms1 and miR-142-3p was detected by qRT-PCR. (E) miRDB predicted the complementary binding sites of miR-142-3p and MST1, and the targeting relationship was validated by luciferase reporter assay. (F) The abundance of miR-142-3p and MST1 was detected by qRT-PCR. (G) The binding of miR-142-3p with circRbms1 and MST1 was proved by RNA pull-down assay. (H, I) MST1 was detected in control (AAV9-shNC), AAV9-shcircRbms1 and AAV9-shcircRbms1 + anti-miR-142-3p group by qRT-PCR (H) and western blot (I). Data are presented as mean ± SD from three independent experiments. $^{**}P < 0.01$, $^{***}P < 0.001$.

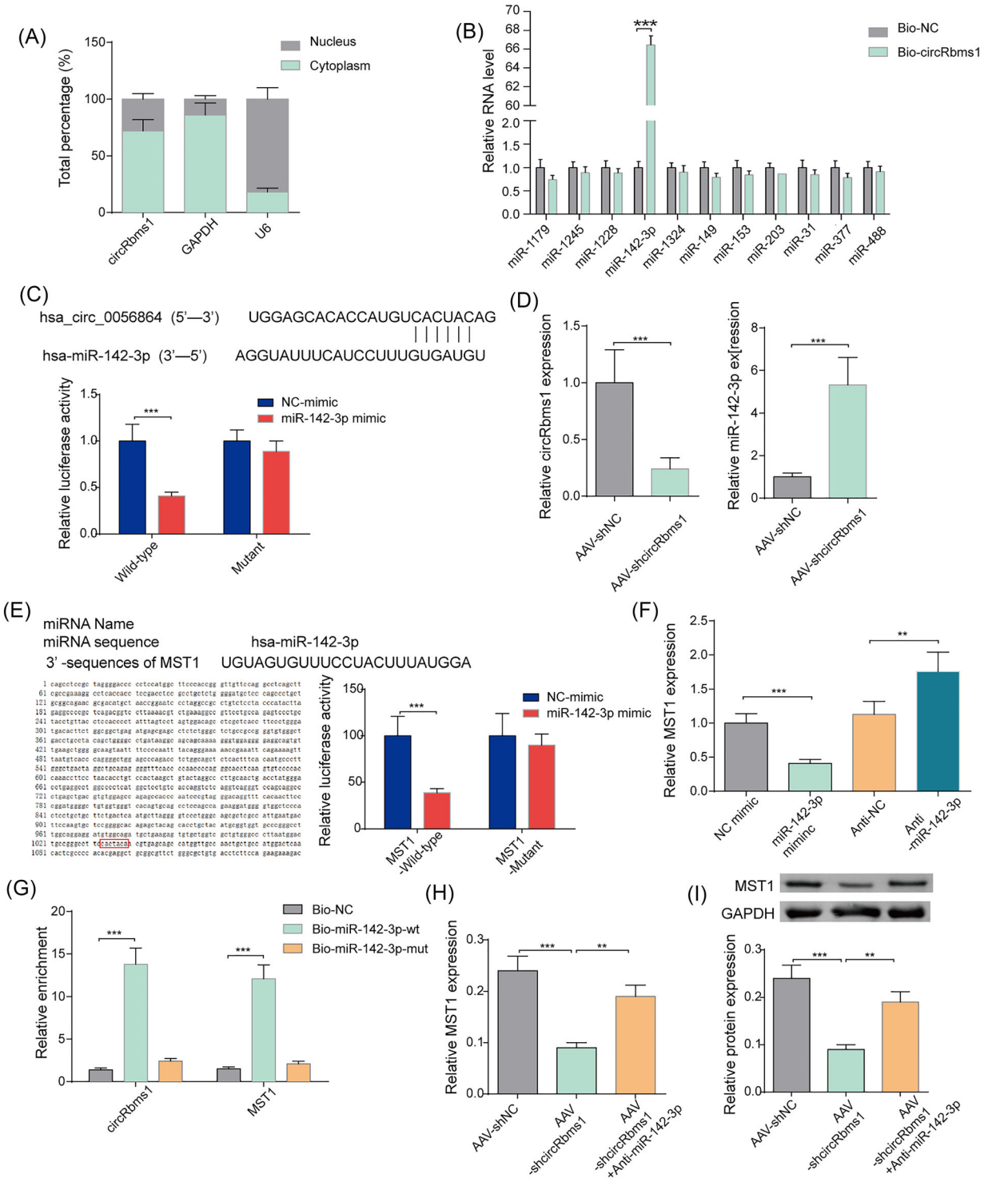

Figure 3 Loss of circRbms1 protected cardiomyocytes against A/R-induced pyroptosis via targeting miR-142-3p/MST1 axis. Cells were treated with A/R. (A–C) The expression levels of circRbms1 (A), miR-142-3p (B) and MST1 (C) were detected at 0, 15, 30, 60 min post treatment. (D) Cells were exposed to A/R and treated with shcircRbms1, shcircRbms1 + anti-miR-142-3p or AAV9-shcircRbms1 + MST1. The expression of caspase-1 was detected by immunofluorescence and statistical results were listed. (E, F) Pyroptosis-related markers, caspase-1, cleaved caspase-1, NLRP3, IL-1β and IL-18 were detected by qRT-PCR (E) and western blot (F). Data are presented as mean ± SD from three independent experiments. $*P < 0.05$, $**P < 0.01$, $***P < 0.001$.

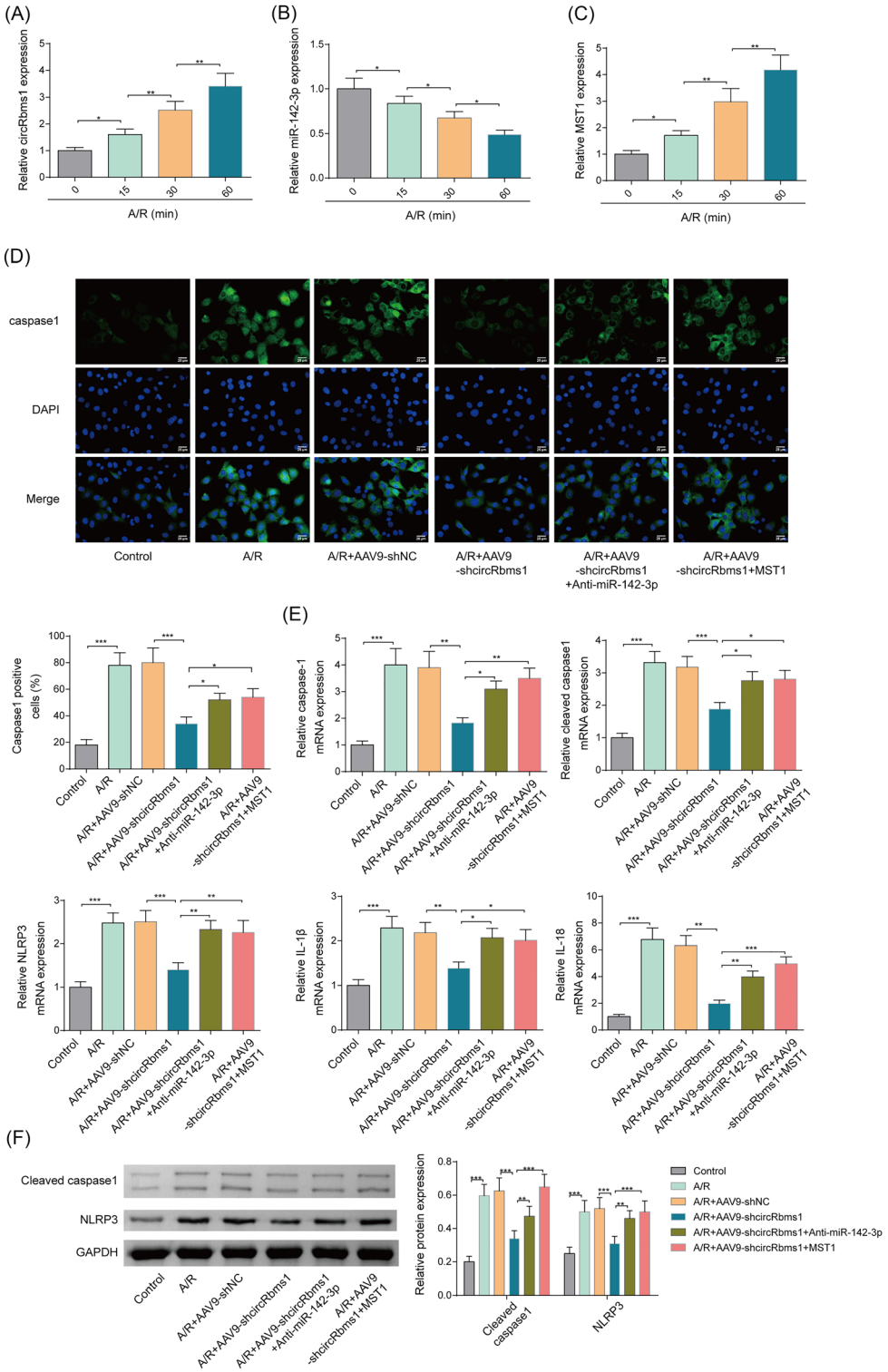

DOI: 10.1002/ehf2.14673

fluorescence activity showed that knocking down circRbms1 reduced caspase-1 fluorescence activity. However, inhibiting miR-142-3p or overexpressing MST1 increased fluorescence activity (*Figure 3D*). We also performed qRT-PCR analysis to determine the expression levels of pyroptosis-related biomarkers. Our results showed that the expression patterns of pyroptosis-related biomarkers were similar. Knocking down circRbms1 reduced their expression levels, while inhibiting miR-142-3p or overexpressing MST1 increased their expression (*Figure 3E*). Western blot analysis was performed to further validate the expression of pyroptosis-related molecules, and the results were consistent with those of qRT-PCR analysis (*Figure 3F*). These experiments demonstrated that silencing of circRbms1 significantly alleviated A/R-induced pyroptosis in cardiomyocytes. However, this protective effect was significantly reversed when miR-142-3p was simultaneously inhibited or when MST1 was overexpressed.

Loss of CircRbms1 protects cardiomyocytes against A/R-induced weakened autophagic status and poor proliferative capacity via targeting miR-142-3p/MST1 axis

We assessed cell proliferation by performing IF detection of Ki67 fluorescence activity. Our results showed an increase in cell proliferation after knocking down circRbms1. However, when miR-142-3p was inhibited or MST1 was overexpressed, proliferation levels were suppressed (*Figure 4A*). Changes in the number of autophagosomes in cardiomyocytes were observed using transmission electron microscopy. Our results showed an increase in the number of autophagosomes after knocking down circRbms1. However, when miR-142-3p was inhibited or MST1 was overexpressed, the number of autophagosomes decreased (*Figure 4B*). We performed IF detection of LC3 fluorescence activity and found an increase in LC3 levels after knocking down circRbms1. However, when miR-142-3p was inhibited or MST1 was overexpressed, LC3 levels decreased (*Figure 4C*). The expression levels of autophagy-related molecules were further validated using western blot. The results were consistent with those of electron microscopy and immunofluorescence experiments (*Figure 4D*). The experiments showed that silencing circRbms1 led to a significant reduction in the inhibitory effect of A/R on cardiomyocyte proliferation and increased autophagy in cardiomyocytes. However, these effects were significantly reversed when miR-142-3p was inhibited or MST1 was overexpressed.

circRbms1 enhances the mRNA stability of MST1 via recruiting IGF2BP2

A schematic diagram was created to illustrate the circRbms1 pull-down in cardiomyocytes (*Figure 5A*). Western blot was performed to determine the protein levels of IGF2BP1, IGF2BP2, and IGF2BP3 in protein pull-down samples from cardiomyocytes following tagged RNA affinity purification assays. Our results confirmed that IGF2BP2 was a key RNA-binding protein (RBP) that can bind to circRbms1 (*Figure 5B*). The efficiency of circRbms1 pull-down by RIP assay was examined (*Figure 5C*). RIP assay revealed the enrichment of MST1 mRNA in anti-IGF2BP2 antibody (*Figure 5D*). The localization of circRbms1 (green) and IGF2BP2 (red) overlapped as detected by immunofluorescence and FISH (*Figure 5E*). qRT-PCR and western blot revealed that IGF2BP2 inhibition reduced the stability of MST1 mRNA (*Figure 5F,G*). These results suggested a potential regulatory role for circRbms1 in the stability of MST1 mRNA via its interaction with IGF2BP2.

The mechanism of circRbms1's effect on I/R injury is validated in vivo

At the animal level, mice received adenoviruses carrying plasmids by injection as described in the methods. We detected INF/LV (%) and infarct size (% of risk zone). INF/LV and representative images of myocardial tissue in indicated mice showed that cardiac injury was alleviated after knocking down circRbms1. However, the degree of cardiac injury repair was weakened when miR-142-3p was inhibited or MST1 was overexpressed (*Figure 6A,B*). Caspase-1 signal activity was diminished after circRbms1 was inhibited, as indicated by IHC staining. However, when miR-142-3p was inhibited or MST1 was overexpressed, the signal increased (*Figure 6C*). qRT-PCR analysis of pyroptosis-related biomarkers revealed that their expression levels decreased after circRbms1 knockdown. Nonetheless, when miR-142-3p was inhibited or MST1 was overexpressed, their expression levels increased (*Figure 6D*). IF detection of Ki67 demonstrated an increase in cell proliferation following circRbms1 inhibition. When miR-142-3p was inhibited or MST1 was overexpressed; however, proliferation levels were reduced (*Figure 6E*). After inhibiting circRbms1, we detected an increase in LC3 levels using immunofluorescence. When miR-142-3p was inhibited or MST1 was overexpressed, LC3 levels decreased (*Figure 6F*). Western blot analysis revealed a decrease in MST1 expression following circRbms1 inhibition. When miR-142-3p was inhibited or MST1 was overexpressed, MST1 expression increased (*Figure 6G*). Therefore, the effect of circRbms1 on I/R injury mechanism has been validated in vivo.

Discussion

Myocardial I/R injury poses a serious threat to the prognosis of patients with AMI.[11] Therefore, a treatment that can alleviate I/R injury is particularly important for improving the

Figure 4 Loss of circRbms1 protected cardiomyocytes against A/R-induced weakened autophagic status and poor proliferative capacity via targeting miR-142-3p/MST1 axis. Cells were exposed to A/R and treated with shcircRbms1, shcircRbms1 + anti-miR-142-3p or AAV9-shcircRbms1 + MST1. (A) Ki-67 was detected by immunofluorescence. (B) Changes in the number of autophagosomes were quantified by TEM. (C) LC3 activity was detected by immunofluorescence. (D) The expression of autophagy-related molecules, LC3I, LC3II, Beclin1, p62 and MST1 was detected by western blot. Data are presented as mean ± SD from three independent experiments. ***$P < 0.001$.

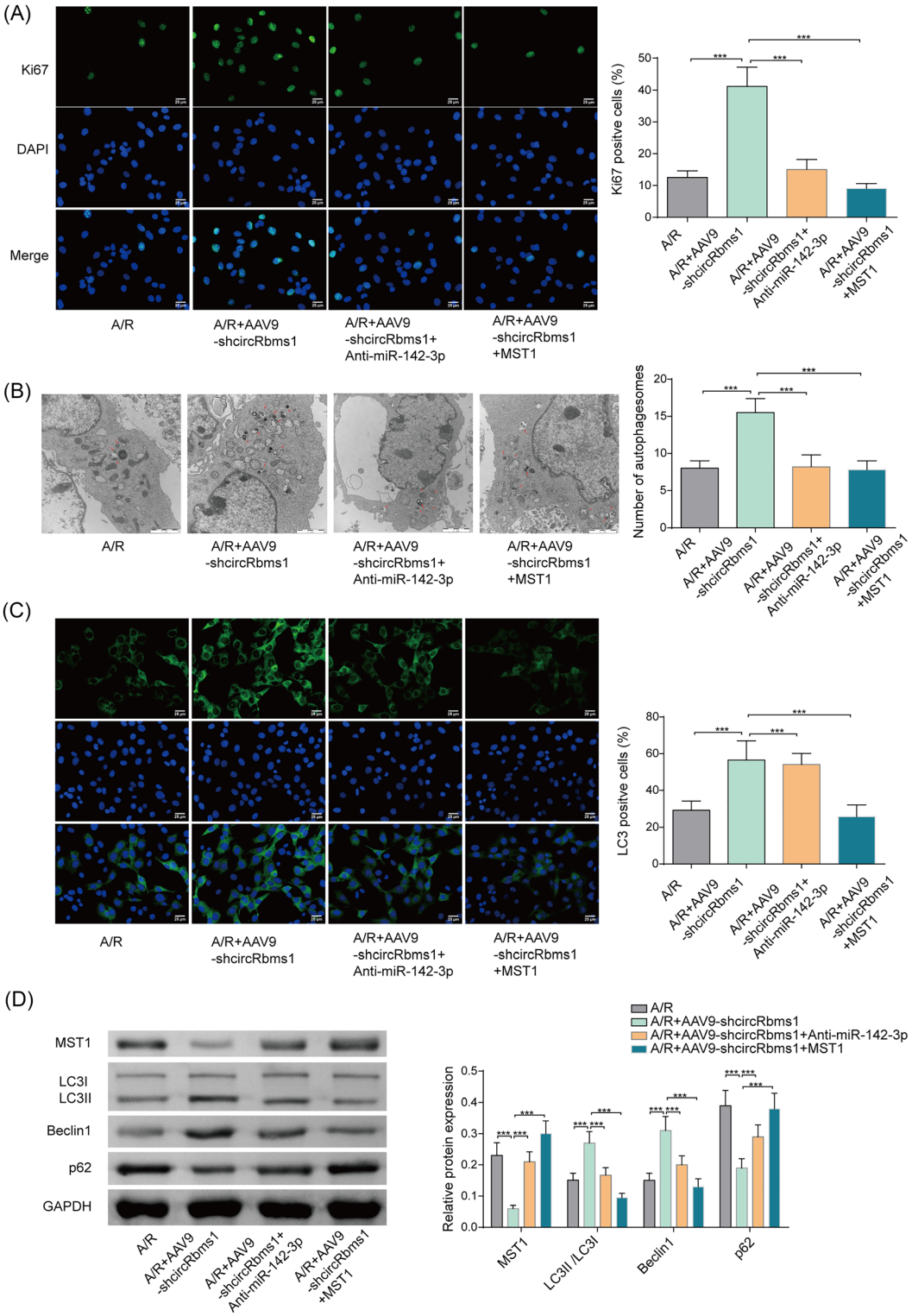

Figure 5 CircRbms1 enhanced the mRNA stability of MST1 via recruiting IGF2BP2. (A) Schematic diagram of circRbms1 pulls down in cardiomyocytes. (B) Western blot analysis of IGF2BP1, IGF2BP2, and IGF2BP3 protein levels in the protein pulldown samples from cardiomyocytes following tagged RNA affinity purification assays. (C) The efficiency of circRbms1 pulled down was examined by RNA immunoprecipitation (RIP) assay. (D) MST1 was detected in cells treated with anti-IgG (control) or anti-IGF2BP2. (E) The localization of circRbms1 (green) and IGF2BP2 (red) was detected by immunofluorescence and RNA-fluorescence in situ hybridization (FISH). (F) MST1 and IGF2BP2 were detected by qRT-PCR in cells treated with si-NC (control) or si-IGF2BP2. (G) Half-life of MST1 mRNA was detected in cells treated with si-NC (control) or si-IGF2BP2. Data are presented as mean ± SD from three independent experiments. $^{**}P < 0.01$, $^{***}P < 0.001$.

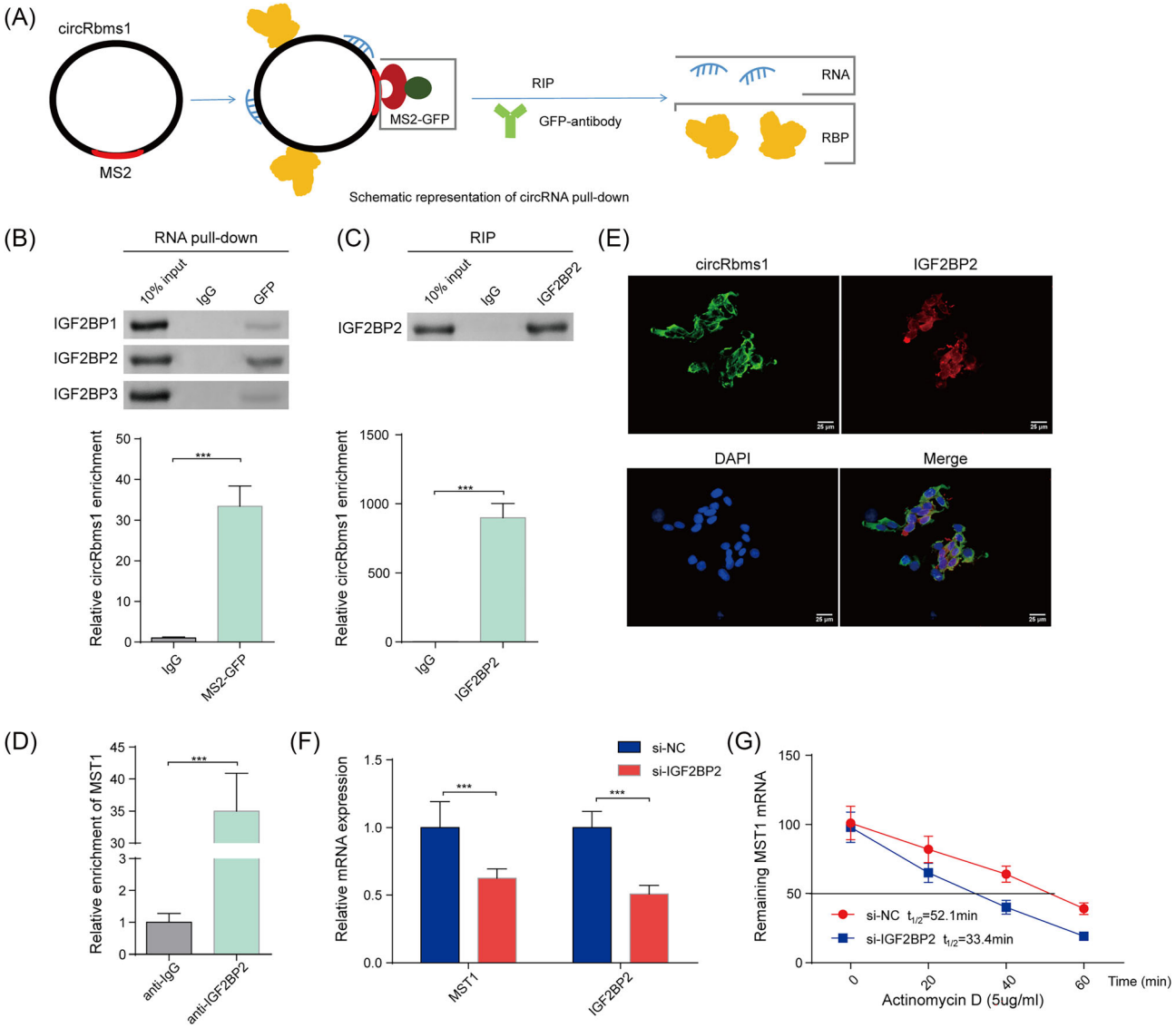

therapeutic effect of AMI.[12] Cell pyroptosis has a significant pro-inflammatory effect. Therefore, compared with other cell programmatic death modes such as apoptosis and autophagy, pyroptosis not only leads to the death of myocardial cells but also leads to the activation of local inflammatory reactions, which further aggravates local tissue damage. This also makes pyroptosis a more important therapeutic target than other programmatic deaths such as apoptosis and autophagy.[13–15] Our previous study revealed that A/R-induced HCMs had increased circRbms1. CircRbms1 served as a sponge for miR-2355-3p and miR-2355-3p targeted MST1. Furthermore, knockout of circRbms1 attenuated cell apoptosis, oxidized stress, and inflammation in A/R-induced HCMs.[7] In this study, knocking down circRbms1 can reduce caspase-1 signal activity and pyroptosis-related biomarkers expression while increasing cell proliferation and LC3 levels. However, the degree of cardiac injury repair was weakened when miR-142-3p was inhibited or MST1 was overexpressed. Therefore, the miR-142-3p/MST1 axis might be the downstream target of circRbms1.

Figure 6 The regulatory axis of circRbms1/MST1 in myocardial I/R injury in vivo. Mice received adenoviruses carrying plasmids by injection as described in methods. After 5 days, the mice were subjected to myocardial I/R (45 min/180 min) and then assigned to 5 groups, sham, I/R, I/R + AAV9-shNC, I/R + AAV9-shcircRbms1, I/R + AAV9-shcircRbms1 + anti-miR-142-3p and I/R + AAV9-shcircRbms1 + MST1. (A) INF/LV (%) and Infract size (% of risk zone) are detected. (B) Representative images of heart tissues in indicated mice. (C) Caspase-1 was detected by IHC staining. (D) Pyroptosis-related biomarkers, NLRP3, IL-1β, and IL-18 were detected by qRT-PCR. (E) Ki-67 was detected by immunofluorescence. (F) LC3 activity was detected by immunofluorescence. (G) MST1 was detected by western blot. Data are presented as mean ± SD from three independent experiments. *$P < 0.05$, ** $P < 0.01$, ***$P < 0.001$.

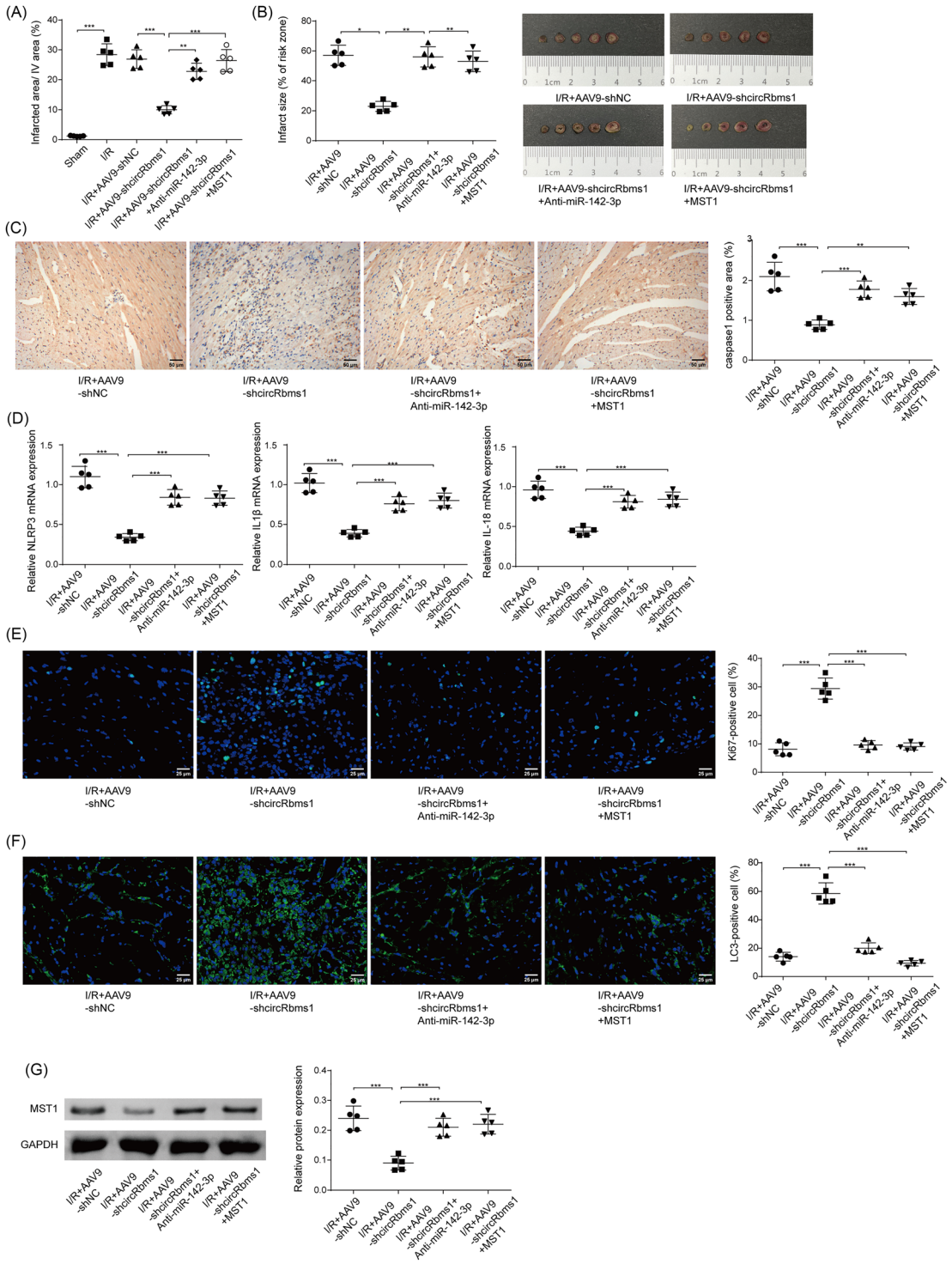

DOI: 10.1002/ehf2.14673

CircRbms1 plays an important role in a variety of cardiovascular diseases, including MI. CircRbms1 was up-regulated in the heart tissues of MI mice and hypoxia-induced cardiomyocytes. Hypoxia induced cardiomyocyte injury by suppressing cell viability, migration, and invasion, and promoting apoptosis. Function experiments showed that circRbms1 overexpression aggravated hypoxia-induced cardiomyocyte injury, while its silencing relieved cardiomyocyte injury induced by hypoxia.[16] Another study found that circRbms1 mediated H/R induced cell injury by targeting miR-2355-3p/MST1 axis. It was also found that circRbms1 knockdown attenuated cardiac function, cell apoptosis, oxidative stress injury, and inflammation response through regulating miR-2355-3p/MST1 axis in I/R mouse model.[7] CircRNA has diverse regulatory downstream molecular patterns. On the one hand, it acts as a miRNA sponge to regulate the expression of target genes; on the other hand, it can recruit RNA-binding proteins to affect the stability of downstream mRNA. In the current study, circRbms1 also exerted regulatory roles by two ways. CircRbms1 served as a miRNA sponge for miR-142-3p to enhance MST1 expression as well as enhanced the mRNA stability of MST1 via recruiting IGF2BP2.

MiR-142-3p is an inflammatory miRNA that plays a dual role in the immune and central nervous systems. Dysregulated miR-142-3p has been implicated in multiple cardiovascular diseases and was significantly down-regulated in coronary microembolization (CME)-induced myocardial injury.[17] Moreover, miR-142-3p overexpression alleviated hypoxia/reoxygenation-induced apoptosis and fibrosis of cardiomyocytes through targeting HMGB1.[18] Based on the previous studies mentioned above, we speculated that miR-142-3p may also be involved in the regulation of circRbms1 in myocardial injury. In this study, we reported for the first time that miR-142-3p was reduced in A/R-induced HCMs. Additionally, miR-142-3p was found to alleviate A/R-induced cell pyroptosis and enhance autophagy.

MST1 (mammalian sterile 20-like kinase 1) was an upstream component of the Hippo pathway that regulated cell growth and death responses in various cell types.[19] In the heart, MST1 not only induced apoptosis but also regulated autophagy.[20] MST1 has been shown to impair protein quality control mechanisms in the heart through inhibition of autophagy. Stress-induced activation of MST1 in cardiomyocytes promoted accumulation of p62 and aggresome formation, accompanied by the disappearance of autophagosomes.[21] Cardiomyocyte-specific MST1 gene knockout can reduce Ang II-induced myocardial injury by promoting cardiomyocyte autophagy. This mechanism may be related to the inhibition of the ROS-mediated JNK signalling pathway.[22] Our research revealed that MST1 expression was elevated in A/R-induced HCMs, corroborating findings from prior research. Hence, we have described a novel mechanism of circRbms1 during A/R-induced cell injury by targeting miR-142-3p/MST1 and by directly modulating MST1's stability. Among increasing data describing a role for circRNA as a link between autophagic status and myocardial I/R injury, our work may contribute towards further supplying attractive potential target for therapeutic approaches.

However, there are also still some limitations to this investigation. The relationship between circRbms1 and prognosis in clinical scenarios remains to be urgently explored. Besides, whether the regulatory axis of circRbms1 would be applicable to more other mammals, such as rats, is required to be further validated. Not all significant signalling pathways were discussed. We will supplement and improve these works with subsequent research.

Acknowledgements

This study is supported by National Natural Science Foundation of China (82060344, 82360383, and 82360384), Natural Science Foundation of Jiangxi Province (20224ACB216002, 20202BABL216032, and 20202BABL206145), Key Research and Development Project of Jiangxi Province (20212BBG73020).

Conflict of interest

The authors declare no conflict of interest.

References

1. He J, Liu D, Zhao L, Zhou D, Rong J, Zhang L, *et al*. Myocardial ischemia/reperfusion injury: Mechanisms of injury and implications for management (review). *Exp Ther Med* 2022;**23**:430. doi:10.3892/etm.2022.11357
2. Heusch G. Myocardial ischaemia-reperfusion injury and cardioprotection in perspective. *Nat Rev Cardiol* 2020;**17**:773-789. doi:10.1038/s41569-020-0403-y
3. Li X, Liu M, Sun R, Zeng Y, Chen S, Zhang P. Protective approaches against myocardial ischemia reperfusion injury. *Exp Ther Med* 2016;**12**:3823-3829. doi:10.3892/etm.2016.3877
4. Zheng J, Chen P, Zhong J, Cheng Y, Chen H, He Y, *et al*. HIF-1alpha in myocardial ischemia-reperfusion injury (review). *Mol Med Rep* 2021;**23**:352. doi:10.3892/mmr.2021.11991
5. Chen LL. The expanding regulatory mechanisms and cellular functions of circular RNAs. *Nat Rev Mol Cell Biol*

2020;**21**:475-490. doi:10.1038/s41580-020-0243-y
6. Hausenloy DJ, Yellon DM. Ischaemic conditioning and reperfusion injury. *Nat Rev Cardiol* 2016;**13**:193-209. doi:10.1038/nrcardio.2016.5
7. Liang Y, Jie H, Liu Q, Li C, Xiao R, Xing X, *et al*. Knockout of circRNA single stranded interacting protein 1 (circRBMS1) played a protective role in myocardial ischemia-reperfusion injury though inhibition of miR-2355-3p/mammalian Sterile20-like kinase 1 (MST1) axis. *Bioengineered* 2022;**13**:12726-12737. doi:10.1080/21655979.2022.2068896
8. Shi H, Gao Y, Dong Z, Yang J, Gao R, Li X, *et al*. GSDMD-mediated cardiomyocyte pyroptosis promotes myocardial I/R injury. *Circ Res* 2021;**129**:383-396. doi:10.1161/CIRCRESAHA.120.318629
9. Ma S, Wang Y, Chen Y, Cao F. The role of the autophagy in myocardial ischemia/reperfusion injury. *Biochim Biophys Acta* 2015;**1852**:271-276. doi:10.1016/j.bbadis.2014.05.010
10. Zhang CL, Long TY, Bi SS, Sheikh SA, Li F. CircPAN3 ameliorates myocardial ischaemia/reperfusion injury by targeting miR-421/Pink1 axis-mediated autophagy suppression. *Lab Invest* 2021;**101**:89-103. doi:10.1038/s41374-020-00483-4
11. Yang M, Linn BS, Zhang Y, Ren J. Mitophagy and mitochondrial integrity in cardiac ischemia-reperfusion injury. *Biochim Biophys Acta Mol Basis Dis* 2019;**1865**:2293-2302. doi:10.1016/j.bbadis.2019.05.007
12. Neri M, Riezzo I, Pascale N, Pomara C, Turillazzi E. Ischemia/reperfusion injury following acute myocardial infarction: A critical issue for clinicians and forensic pathologists. *Mediators Inflamm* 2017;**2017**:7018393. doi:10.1155/2017/7018393
13. Del RD, Amgalan D, Linkermann A, Liu Q, Kitsis RN. Fundamental mechanisms of regulated cell death and implications for heart disease. *Physiol Rev* 2019;**99**:1765-1817. doi:10.1152/physrev.00022.2018
14. Sun T, Ding W, Xu T, Ao X, Yu T, Li M, *et al*. Parkin regulates programmed necrosis and myocardial ischemia/reperfusion injury by targeting cyclophilin-D. *Antioxid Redox Signal* 2019;**31**:1177-1193. doi:10.1089/ars.2019.7734
15. Xu T, Ding W, Ao X, Chu X, Wan Q, Wang Y, *et al*. ARC regulates programmed necrosis and myocardial ischemia/reperfusion injury through the inhibition of mPTP opening. *Redox Biol* 2019;**20**:414-426. doi:10.1016/j.redox.2018.10.023
16. Liu B, Guo K. CircRbms1 knockdown alleviates hypoxia-induced cardiomyocyte injury via regulating the miR-742-3p/FOXO1 axis. *Cell Mol Biol Lett* 2022;**27**:31. doi:10.1186/s11658-022-00330-y
17. Su Q, Lv X, Ye Z, Sun Y, Kong B, Qin Z, *et al*. The mechanism of miR-142-3p in coronary microembolization-induced myocardiac injury via regulating target gene IRAK-1. *Cell Death Dis* 2019;**10**:61. doi:10.1038/s41419-019-1341-7
18. Wang Y, Quyang M, Wang Q, Jian Z. MicroRNA-142-3p inhibits hypoxia/reoxygenation-induced apoptosis and fibrosis of cardiomyocytes by targeting high mobility group box 1. *Int J Mol Med* 2016;**38**:1377-1386. doi:10.3892/ijmm.2016.2756
19. Wang S, Zhou L, Ling L, Meng X, Chu F, Zhang S, *et al*. The crosstalk between hippo-YAP pathway and innate immunity. *Front Immunol* 2020;**11**:323. doi:10.3389/fimmu.2020.00323
20. Maejima Y, Zablocki D, Nah J, Sadoshima J. The role of the hippo pathway in autophagy in the heart. *Cardiovasc Res* 2023;**118**:3320-3330. doi:10.1093/cvr/cvac014
21. Maejima Y, Kyoi S, Zhai P, Liu T, Li H, Ivessa A, *et al*. Mst1 inhibits autophagy by promoting the interaction between Beclin1 and Bcl-2. *Nat Med* 2013;**19**:1478-1488. doi:10.1038/nm.3322
22. Wang X, Song Q. Mst1 regulates post-infarction cardiac injury through the JNK-Drp1-mitochondrial fission pathway. *Cell Mol Biol Lett* 2018;**23**:21. doi:10.1186/s11658-018-0085-1